Hybrid Spectral FDTD/TD-VFz method for analysis of periodic absorbers

Samuel Gaucher, Christophe Guiffaut, Alain Reineix, Olivier Cessenat

Hybrid Spectral FDTD/TD-VFz method for analysis of periodic absorbers

1st Samuel Gaucher
Gironde/Haute-Vienne
CEA CESTA/XLIM
Le Barp/Limoges, France
samuel.gaucher@xlim.fr

2nd Christophe Guiffaut
Haute-Vienne
XLIM
Limoges, France
christophe.guiffaut@xlim.fr

3rd Alain Reineix
Haute-Vienne
XLIM
Limoges, France
alain.reineix@xlim.fr

4th Olivier Cessenat
Gironde
CEA CESTA
Le Barp, France
olivier.cessenat@cea.fr

Abstract—The Spectral FDTD scheme is combined with the discrete-time time-domain vector fitting decomposition technique to analyze wide-angle ultra-broadband absorbers with polarization-insensitive characteristics.

Index Terms—periodic bounday condition, oblique incidence, Spectral FDTD, time-domain vector fitting, ultra-broadband absorbers, polarization-insensitive

I. INTRODUCTION

Periodic absorbers are often required for several applications. Their characterization versus frequency often requires numerical modeling. Thus, periodic boundary conditions (PBC) are applied to simulate only one pattern rather than the entire structure. For this purpose, the efficiency, wideband and simple finite-difference time-domain (FDTD) method is used to compute the electromagnetic (EM) fields. However, PBCs for oblique plane wave illumination cannot be performed with the standard FDTD scheme. A modified FDTD scheme such as Spectral FDTD (SFDTD) [1] [2] method is a good candidate because few changes are required to adapt a FDTD solver and its numerical models. Moreover no additional constraint is needed on the CFL criterion. However the horizontal wavenumber is fixed with this approach and not the incident angle. As a result, unwanted evanescent and horizontal modes [1] are excited leading to a low time convergence and then inaccurate spectral responses. To overcome this problem, we propose to combine the SFDTD method with the discrete-time time-domain vector fitting (TD-VFz) [3] to identify the eigen-frequencies of the periodic structure. In addition to efficiency solve the resonance problem, the frequency versus wavenumber mapping is straightforwardly transformed to frequency versus incident angle one by using the TD-Vfz rational transfer function. To validate the proposed method, angular-stable ultra-broadband absorbers from literature with polarization-insensitive characteristics are computed with the XLIM laboratory home-made Temsi-fd solver [4]. For structures composed of a dielectric substrate with constant complex permittivity, a dispersive Debye model is designed by optimization process to approach it over a desired wideband.

II. HYBRID SPECTRAL-FDTD/TD-VFz METHOD

A. Spectral-FDTD review

Let us consider a (l_x, l_y) periodicity in the (x, y) directions with a z-propagation of a Gaussian incident wave. First, an

arbitrary azimuth angle is chosen to $\varphi = \varphi_0$. Then, the horizontal wavenumber depends on the angular frequency $\omega = 2\pi f$ and the elevation angle θ as $k_h = \omega \sin\theta/c_0$ where c_0 is the speed of light in free space. The term k_h is fixed for one simulation of the SFDTD method. The constant components k_x and k_y of the plane wave vector k are deduced as a function of the azimuth angle and the constant horizontal wavenumber

$$k_x = k_h \cos\varphi_0, \quad k_y = k_h \sin\varphi_0. \tag{1}$$

By fixing them, simple time-domain PBC are found for $\Psi = E$ or H

$$\Psi(x, y, z, t) = \Psi\left(x + ml_x, y + nl_y, z, t\right) e^{j(k_x ml_x + k_y nl_y)}, \tag{2}$$

where m and n are any integers. Then, SFDTD scheme is exactly the same as the FDTD one with complex E-H fields unknowns instead of real for the latter. We deduce by the expression $\theta(\omega) = \arcsin\dfrac{k_h}{k_0}$ that different frequencies correspond to different incident angles, and for a positive real incidence, the condition $k_0 \geq k_h$ must be verified. In other words, this is referred to the plane wave region if $f \geq f_c$ else to the evanescent wave region, where

$$f_c = \frac{c_0 k_h}{2\pi} \tag{3}$$

is the cut-off frequency. When both the plane and evanescent wave region are excited simultaneously by the SFDTD method, surface waves are guided along horizontal directions at some frequencies. Thus, the energy of a horizontal wave continuously re-enters the computational domain through the PBC instead of being absorbed by the top and bottom convolution perfectly matched layers (CPML) [1]. As a result, a resonance behavior occurs: temporal data do not converge and an accurate spectral response cannot be obtained by discrete Fourier transform (DFT).

B. TD-VFz method in Matlab post-processing

To obtain a correct spectral reflection coefficient $\mathcal{R}$, the ratio between the input (excitation) and output (real part of the reflected field) response is decomposed with TD-VFz [3], as a rational transfer function

$$\mathcal{R}(z = \exp[j\omega\Delta_t]) = d + \sum_{n=1}^{M} \frac{r_n}{1 - z^{-1}s_n}, \tag{4}$$

where d is a constant, r_n and s_n are the complex residues and poles respectively and Δ_t is the time sample. The TD-VFz

extrapolation algorithm is an iterative finding poles method: conjugated complex poles are initialized inside the unit circle (linearly distributed near the unit circle boundary) and the new poles are deduced from an eigenvalue problem so-called 'poles relocation'. When poles have converged, the residues are obtained as the solution in the least squares sense of an oversized linear system. An interesting point consists in the eigen-frequencies identification. When (4) gives poles on the unit circle boundary, resonances occur and eigen-frequencies are identified.

C. Mapping $\mathcal{R}(0 < k_h, f)$ to $\mathcal{R}(0 < \theta, f)$

The normal incidence case $\theta = 0°$ is trivial and corresponds to $k_h = 0$. To deal with oblique incident angles for the frequency band $[0 < f_{min}, f_{max}]$ and incident angle band $[0 < \theta_{min}, \theta_{max}]$ of interest, we first calculate the extremum horizontal wavenumber as

$$k_{h_{max}} = \frac{2\pi f_{max}}{c_0} \sin\theta_{max}, \ k_{h_{min}} = \frac{2\pi f_{min}}{c_0} \sin\theta_{min}. \tag{5}$$

To compute the reflection coefficient as a function of the incident angle, we run the FDTD simulation for the N samples of k_h^i with the fixed azimuth angle $\varphi = \varphi_0$

$$k_h^i = k_{h_{min}} + i\frac{k_{h_{max}} - k_{h_{min}}}{N-1}, \ i = 0, \dots, N-1, \tag{6}$$

by using (1) to determine the phase values in the PBC formulation (2). Then, each k_h^i sample is extrapolated by the M-order TD-VFz algorithm to obtain the M residues r_n^i, the M poles s_n^i and the constant d^i. After that, an incident angle-reconstruction is applied. For a given angle $\theta_{min} < \theta_j \leq \theta_{max}$, we compute the N frequencies

$$f^i = \frac{ck_h^i}{2\pi \sin\theta_j}, \ i = 0, \dots, N-1. \tag{7}$$

The reflection coefficient $\mathcal{R}$ evaluated at angle θ_j is calculated with the transfer function (4) for all frequencies f^i

$$\mathcal{R}(f^i, \theta_j) = d^i + \sum_{n=1}^{M} \frac{r_n^i}{1 - \exp\left[-j2\pi f^i \Delta_t\right]s_n^i}. \tag{8}$$

As frequencies are imposed by the formula (7), the Lagrange interpolation is used to obtain the reflection coefficient at the desired frequencies. Assuming a desired frequency $f^i \leq \tilde{f} \leq f^{i+1}$, the reflection coefficient for the angle θ_j and frequency $\tilde{f}$ is given by

$$\mathcal{R}(\tilde{f}, \theta_j) = \frac{f^{i+1} - \tilde{f}}{f^{i+1} - f^i}\mathcal{R}(f^i, \theta_j) + \frac{\tilde{f} - f^i}{f^{i+1} - f^i}\mathcal{R}(f^{i+1}, \theta_j). \tag{9}$$

III. DEBYE MODEL TO APPROXIMATE A CONSTANT COMPLEX PERMITTIVITY

A. One pole Debye model

Several metamaterials are specified by a constant complex permittivity

$$\epsilon = \epsilon_0 \left(\epsilon_r' - j\epsilon_r''\right), \ \epsilon_r', \ \epsilon_r'' > 0. \tag{10}$$

[5] proposed a dispersive one pole Debye model with a conductivity parameter to approach it over a desired wideband. Then, the Debye relative complex permittivity reads

$$\epsilon_r = \epsilon_\infty + \frac{\epsilon_s - \epsilon_\infty}{1 + j\omega\tau_0} - \frac{j\sigma}{\omega\epsilon_0} = \epsilon_{r_{debye}}' - j\epsilon_{r_{debye}}'', \tag{11}$$

where ϵ_∞ is the infinite frequency permittivity, ϵ_s is the static permittivity et τ_0 is the relaxation time. An efficient setting of (11) over a desired wideband f_{min} to f_{max} is obtained by adjusting the imaginary and real parts of (11) with (10) at the frequencies f_{min} and f_{max}. For example for f_{min}

$$K\epsilon_r' = \epsilon_\infty + \frac{\epsilon_s - \epsilon_\infty}{1 + (2\pi f_{min}\tau_0)^2}, \tag{12}$$

$$K\epsilon_r'' = \frac{(\epsilon_s - \epsilon_\infty)2\pi f_{min}\tau_0}{1 + (2\pi f_{min}\tau_0)^2} + \frac{\sigma}{2\pi f_{min}\epsilon_0}, \tag{13}$$

where the approximation factor $K > 1$ should be close to one. Two other equations follow by replacing f_{min} by f_{max} and K by $K_2 = 1/K$ in (12) and (13). We obtain a nonlinear system with four unknons ϵ_∞, ϵ_s, τ_0 and σ which can be solved with the 'fminsearch' Matlab function. To determine the optimum approximation factor $\tilde{K}$, 'fminsearch' is applied for several K between 1.001 and 1.2 with a step $\Delta_K = 0.001$. $\tilde{K}$ is determined when the error function $\mathcal{E}$ is minimum i.e

$$\mathcal{E}(\tilde{K}) = \min_K \mathcal{E}(K), \tag{14}$$

with

$$\mathcal{E}(K) = \max\left(\|\mathcal{A}(K)\|_{L^\infty}, \|\mathcal{B}(K)\|_{L^\infty}\right), \tag{15}$$

$$\mathcal{A}(K) = \epsilon_{r_{debye}}'(K) - \epsilon_r', \tag{16}$$

$$\mathcal{B}(K) = \epsilon_{r_{debye}}''(K) - \epsilon_r'' \tag{17}$$

where the norm L^∞ in (15) is taken on a 100 samples discrete frequency interval of $[f_{min}, f_{max}]$. Finally, the dispersive one pole Debye model now obtained, the JE convolution (JEC) FDTD method [6] is used to compute the EM fields in the unit cell.

B. Examples

1) Flame Resistant 4 (FR4): The FR4 relative permittivity is given by

$$\epsilon_r = 4.3 - j0.025. \tag{18}$$

For the FR4 case, we have $\epsilon_r' = 4.3$ and $\epsilon_r'' = 0.025$. We want to find the four parameters ϵ_∞, ϵ_s, τ_0 and σ of (11) to approach (18) over the frequency band $f_{min} = 0.5$ GHz to $f_{max} = 20$ GHz. The minimum of the error function $\mathcal{E}$ is attained for $\tilde{K} = 1.006$ i.e our optimization process has given this optimum approximation factor where the Matlab function 'fminsearch' returns

$$\epsilon_\infty^{FR4} = 4.26291, \tag{19}$$

$$\epsilon_s^{FR4} = 4.325977, \tag{20}$$

$$\tau_0^{FR4} = 0.169.10^{-10} \ s, \tag{21}$$

$$\sigma^{FR4} = 6.0669.10^{-4} \ S/m. \tag{22}$$

Fig. 1 and Fig. 2 respectively show the real part and imaginary part of the Debye relative permittivity obtained with the parameters (19)-(22). Very good agreement with theory is observed over the desired frequency band.

2) Polymethacrylimide (PMI): The PMI relative permittivity is given by $\epsilon_r = 1.06(1 - j0.005)$. For the desired frequency band $f_{min} = 3$ GHz to $f_{max} = 40$ GHz, our optimization process has given the optimum approximation factor $\tilde{K} = 1.004$ where the Matlab function 'fminsearch' returns $\epsilon_\infty^{PMI} = 1.052899$, $\epsilon_s^{PMI} = 1.064432$, $\tau_0^{PMI} = 6.900626.10^{-12} \ s$ and $\sigma^{PMI} = 6.41903.10^{-4} \ S/m$.
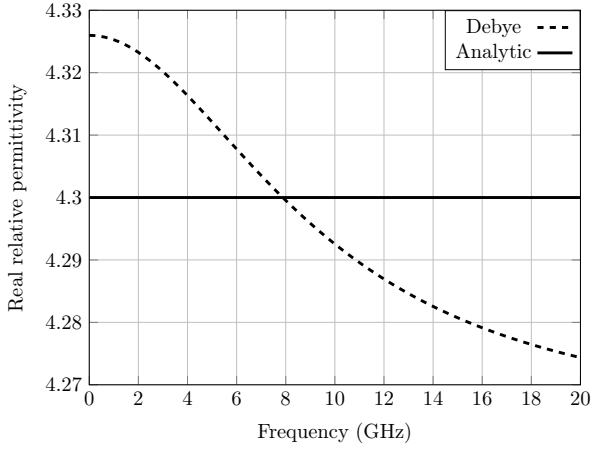
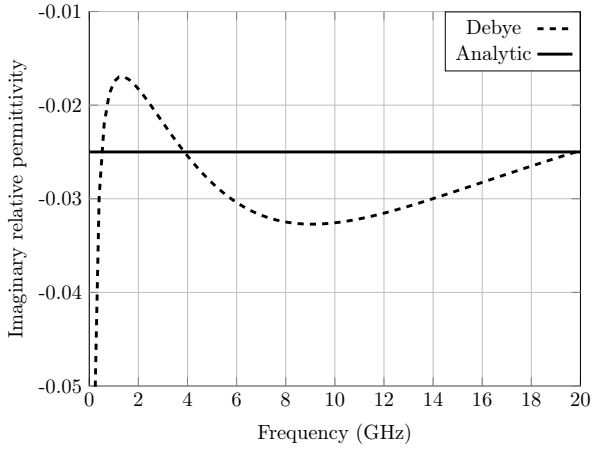Fig. 1. Real part of the FR4 Debye relative permittivity compared with theory.

Fig. 2. Imaginary part of the FR4 Debye relative permittivity compared with theory.

3) Polyethylene glycol terephthalate (PET): The PET relative permittivity is given by $\epsilon_r = 3.0(1 - j0.06)$. For the desired frequency band $f_{min} = 3$ GHz to $f_{max} = 40$ GHz, our optimization process has given the optimum approximation factor $\tilde{K} = 1.045$ where the Matlab function 'fminsearch' returns $\epsilon_\infty^{PET} = 2.774121$, $\epsilon_s^{PET} = 3.140665$, $\tau_0^{PET} = 6.647.10^{-12}$ s and $\sigma^{PET} = 0.02384704$ S/m.

IV. NUMERICAL RESULTS

For the two numerical examples of this section, SFDTD solver runs with a 2 ns simulation time and TD-VFz with $M = 20$ poles and 10 iterations for the poles convergence.

A. PMI and PET absorber with resistive films

As shown in Fig. 3, the studied absorber [7] is composed of three PMI substrates all separated by a PET film of thickness $t_p = 0.175$ mm covered by a resistive film. Note also a metal ground simulated with perfect electric conductor (PEC) to prevent the transmission of the EM waves. The PMI and PET constant complex permittivities are approached with a one pole Debye model over a wideband from 3 GHz to 40 GHz (the parameters are listed in section III-B). The angular responses are deduced by the methodology of section II-C for $N = 100$ samples of horizontal wavenumber
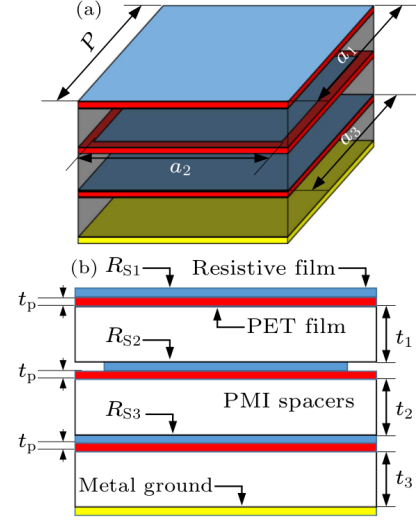

Fig. 3. Pattern geometry of the PMI (white) and PET (red) absorber with resistive films (blue) [7]. $t_1 = 2$ mm, $t_2 = 4$ mm, $t_3 = 3$ mm, $t_p = 0.175$ mm, $P = a_1 = a_3 = 14$ mm, $a_2 = 12.5$ mm.

k_h with $\theta_{max} = 60°$. The FDTD spatial steps are $\Delta_x = \Delta_y = 0.25$ mm and $\Delta_z = 0.125$ mm except for a resistive film or a PET substrate: a resistive film is represented by one FDTD cell whereas a PET substrate by two FDTD cells with $\Delta_z^{PET,film} = 0.0875$ mm. The parameters of the resistive films are $R_{s_1} = 800\Omega/\square$, $R_{s_2} = 450\Omega/\square$ and $R_{s_3} = 250\Omega/\square$ allowing the film conductivities as $\sigma_i = \left(R_{s_i}\Delta_z^{film}\right)^{-1}$. Fig 4 and Fig. 5 show an absorption rate better than 90 % under normal illumination for the frequency band 4.5 GHz to 37 GHz approximately. At low frequencies, more the incident angle increases and more the absorption rate decreases but it remains above 80 % for both TE and TM mode over the frequency band 8-38 GHz.

B. FR4 absorber with ITO films

The studied absorber [8] is composed of a FR4 substrate, covered by thin indium tin oxide (ITO) films. The unit cell geometry is plotted in Fig. 6. The pattern is a Huygens metasurface on three-layers slab impedance metasurface with a metal ground sheet (PEC) to prevent the transmission of EM waves. Dimensions and ITO film conductivities are
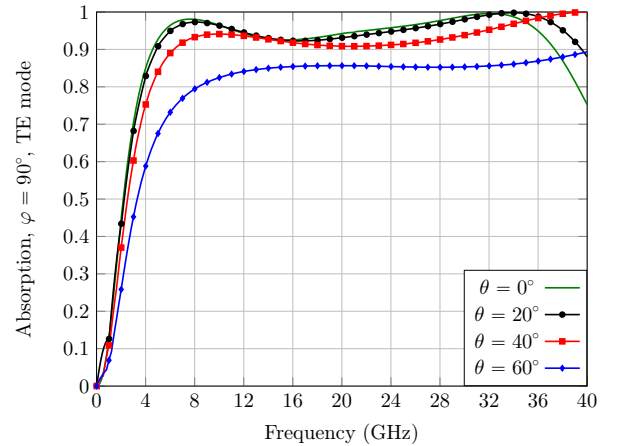

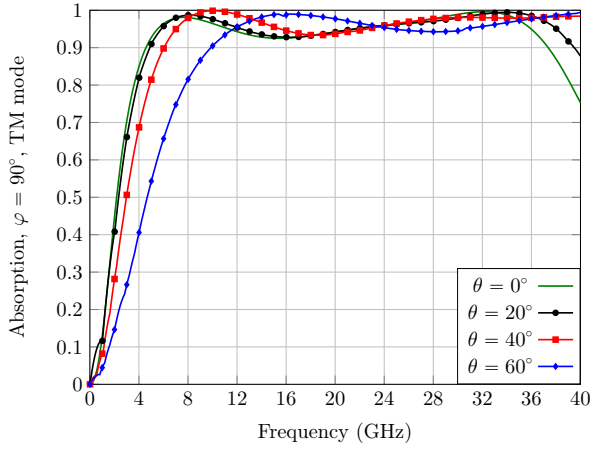Fig. 4. TE mode absorption curve for the PMI/ PET absorber.

Fig. 5. TM mode absorption curve for the PMI/PET absorber.

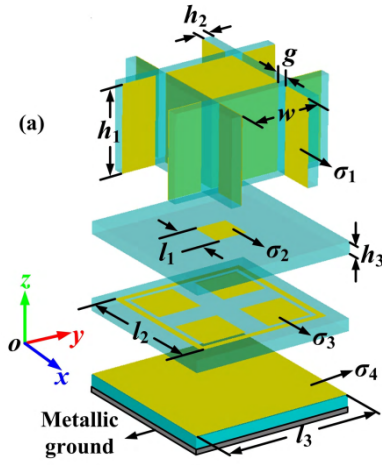Fig. 7. TE mode absorption curve for the FR4/ITO absorber.

Fig. 6. Pattern geometry of the FR4 (blue) absorber with ITO films (yellow) [8]. $h_1 = 21$ mm, $g = h_2 = 2.5$ mm, $w = 20$ mm, $h_3 = 3$ mm, $l_1 = 8$ mm, $l_2 = 35$ mm, $l_3 = 39$ mm, $\sigma_2 = 6.7 \times 10^4$ S/m, $\sigma_1 = \sigma_3 = \sigma_4 = 2.0 \times 10^5$ S/m.

Fig. 8. TM mode absorption curve for the FR4/ITO absorber.

optimized to promote a high absorption rate. The FR4 constant complex permittivity is approached with a one pole Debye model over a wideband from 0.5 GHz to 20 GHz (the parameters are listed in section III-B1). The angular responses are deduced by the methodology of section II-C for $N = 100$ samples of horizontal wavenumber k_h with $\theta_{max} = 60°$. The FDTD spatial steps are all equal to $\Delta = 0.25$ mm. Note that to simulate the $d = 50$ nm thin conductive ITO films, an equivalent conductivity is applied on one FDTD cell i.e $\sigma_i^{cell} = \sigma_i.d/\Delta_z$. Fig. 8 shows that this absorber can achieve an absorption rate better than 90 % over an ultra-broadband 1-18 GHz for the TM mode and for many incident angles. However for the TE mode, the absorption rate is a bit deteriorated at high incidence but remains superior to approximately 75 % over 1-18 GHz as shown in Fig. 7.

V. CONCLUSION

The Spectral FDTD scheme combined with the TD-VFz decomposition is an efficient hybrid approach to analyze periodic structures excited by oblique incident plane waves without reducing the CFL stability criterion of the FDTD
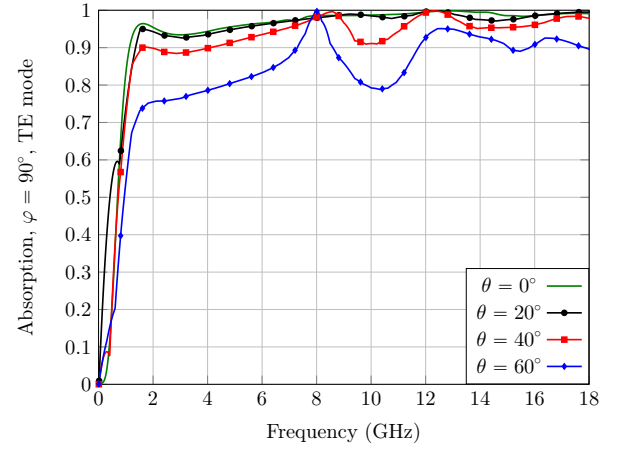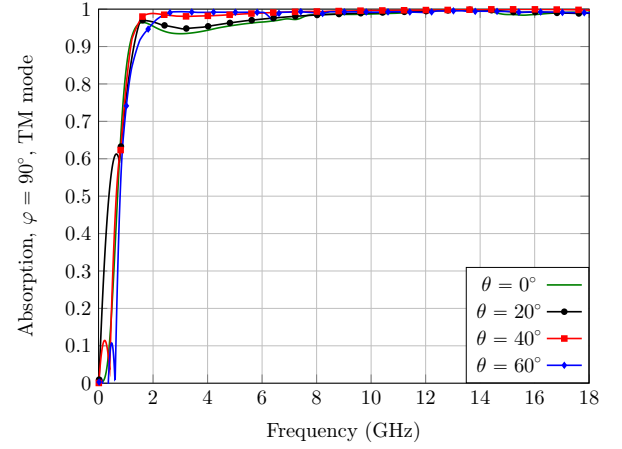
method. The dispersive Debye model is successfully designed with optimization process to simulate two efficient absorbers.

REFERENCES

[1] F. Yang, J. Chen, R. Qiang, and A. Elsherbeni, "A simple and efficient fdtd/pbc algorithm for scattering analysis of periodic structures," *Radio Science*, vol. 42, no. 04, pp. 1–9, 2007.

[2] A. Aminian and Y. Rahmat-Samii, "Spectral fdtd: a novel technique for the analysis of oblique incident plane wave on periodic structures," *IEEE Trans. Antennas Propag.*, vol. 54, no. 6, pp. 1818–1825, 2006.

[3] C.-U. Lei and N. Wong, "Efficient linear macromodeling via discrete-time vector fitting," in *21st International Conference on VLSI Design (VLSID 2008)*. IEEE, 2008, pp. 469–474.

[4] *Time ElectroMagnetic Simulator-Finite Difference Software, TEMSI-FD, CNRS, Univ. Limoges, Limoges, France*, 2006.

[5] R. Luebbers, "Lossy dielectrics in fdtd," *IEEE transactions on antennas and propagation*, vol. 41, no. 11, pp. 1586–1588, 1993.

[6] Q. Chen, M. Katsurai, and P. H. Aoyagi, "An fdtd formulation for dispersive media using a current density," *IEEE Transactions on Antennas and Propagation*, vol. 46, no. 11, pp. 1739–1746, 1998.

[7] P. Chen, X. Kong, J. Han, W. Wang, K. Han, H. Ma, L. Zhao, and X. Shen, "Wide-angle ultra-broadband metamaterial absorber with polarization-insensitive characteristics," *Chinese Physics Letters*, vol. 38, no. 2, p. 027801, 2021.

[8] C.-Y. Wang, J.-G. Liang, T. Cai, H.-P. Li, W.-Y. Ji, Q. Zhang, and C.-W. Zhang, "High-performance and ultra-broadband metamaterial absorber based on mixed absorption mechanisms," *IEEE Access*, vol. 7, pp. 57 259–57 266, 2019.